Puri, S and Morrey, D

A comparison of one and two-sided Krylov-Arnoldi projection methods for fully coupled, damped structural-acoustic analysis.

Puri, S and Morrey, D (2013) A comparison of one and two-sided Krylov-Arnoldi projection methods for fully coupled, damped structural-acoustic analysis. *Journal of Computational Acoustics*, 21 (2). pp. 1350004.

Doi: 10.1142/S0218396X13500045

– **manuscript No.**
(will be inserted by the editor)

R Srinivasan Puri · Denise Morrey

A comparison of one and two-sided Krylov-Arnoldi projection methods for fully coupled, damped structural-acoustic analysis

Received: date / Revised version: date

Abstract The two-sided second order Arnoldi algorithm is used to generate a reduced order model of two test cases of fully coupled, acoustic interior cavities, backed by flexible structural systems with damping. The reduced order model is obtained by applying a *Galerkin-Petrov* projection of the coupled system matrices, from a higher dimensional subspace to a lower dimensional subspace, whilst preserving the low frequency moments of the coupled system. The basis vectors for projection are computed efficiently using a two-sided second-order Arnoldi algorithm, which generates an orthogonal basis

Department of Mechanical Engineering and Mathematical Sciences, Oxford Brookes University, Wheatley Campus, Wheatley, Oxford OX33 1HX, United Kingdom.

for the second-order Krylov subspace containing moments of the original higher dimensional system.

The first model is an ABAQUS benchmark problem: a 2D, point loaded, water filled cavity. The second model is a cylindrical air-filled cavity, with clamped ends and a load normal to its curved surface. The computational efficiency, error and convergence are analysed, and the two-sided second order Arnoldi method shows better efficiency and performance than the one-sided Arnoldi technique, whilst also preserving the second order structure of the original problem.

1 INTRODUCTION

Modelling of structural-acoustic behaviour of enclosed cavities is a requirement in a wide range of engineering applications, but is of particular interest in the development of automotive and aerospace vehicles. Because of the coupling between the fluid and structural domains in the coupled displacement/pressure *(u/p)* FE/FE formulation [8,24,9,10], the resulting mass and stiffness matrices are un-symmetric. In order to give reasonable prediction the mesh density needed can result in huge model sizes for higher frequency analysis, and hence a significant increase of computational time and expense. This is an even greater concern when optimization is a goal, particularly for fully-coupled analyses. A detailed review of the techniques for structural optimization has been presented by Marburg [12], and this describes approaches and the need for speeding up NVH simulation. Hence there is a need for compact models to undertake fast coupled structural-acoustic analysis.

Earlier work by the authors [17,16,15] has focussed on reduced order modelling techniques based on the use of the first-order, one-sided Arnoldi algorithm to compute the basis vectors for the orthogonal Krylov subspace for the solution of undamped fully-coupled structural-acoustic interior problems. However, for a problem involving an explicit particpation of the damping matrix, this involves a change of state to a first order problem, which results in matrices of twice the order of the original matrices, and a loss of structural preservation in terms of original properties.

This paper focuses on the application of Second Order Krylov-Arnoldi based MOR techniques to structurally damped, fully-coupled structural-acoustic problems. The paper is structured as follows: in section 2, the general framework for model order reduction for second order systems is introduced. In section 3 the Krylov-Arnoldi framework adapted for model order reduction for the coupled damped structural-acoustic problem is described. In section 4 a numerical example from the ABAQUS benchmark manual is solved using both the direct approach in ANSYS FE code and the two-sided second order Arnoldi approach. Computational times, solution accuracy and convergence models are discussed. In section 5 a model of a cylindrical air-filled cavity, with clamped ends and a load normal to its curved surface is analysed using both the one-sided and two-sided second order Arnoldi techniques.

2 APPLICATION OF THE SECOND ORDER KRYLOV SUBSPACE AND MOMENT MATCHING PROPERTIES TO STRUCTURAL-ACOUSTIC PROBLEMS

For a fully enclosed, fully coupled, interior acoustic cavity, the well-known *Eulerian* displacement - pressure *(u/p)* formulation [24,9,10], can be written as:

$$[M_{sa}]\ \ddot{q}(t) + [C_{sa}]\ \dot{q}(t) + [K_{sa}]\ q(t) = \mathbf{F}_{MIsa}\ \mu(t) \tag{1a}$$

$$y(t) = L^T q(t) \tag{1b}$$

and,

$$q(t) = \left\{ \begin{array}{c} u(t) \\ \\ p(t) \end{array} \right\} \tag{2}$$

Where, M_{sa} is the coupled mass matrix, K_{sa} is the coupled structural stiffness matrix, C_{sa} is the damping matrix for the structural-acoustic system; $\mu(t)$ is the input force vector and $\mathbf{F}_{MIsa}$ is the multiple-input structural-acoustic input distribution matrix consisting of F_s and F_a, which denote the input distribution force(s) on the structural domain and constrained acoustic pressure degrees of freedom (DOF's), or purely acoustic excitation, in the form of volume acceleration within the fluid domain respectively. $q(t)$ is the output state variable, comprising of $u(t)$ and $p(t)$, which are the displacements of the structural domain and pressure levels in the acoustic domain respectively.

The structural damping matrix $[C_s]$, is modelled as proportional damping, and is therefore written as:

$$[C_s] = \alpha[M_s] + (\beta)[K_s] \tag{3}$$

where, α is the mass matrix multiplier, and β is the stiffness matrix multiplier.

Earlier work by the authors [17,16,15] has demonstrated the efficiencies to be gained through the application of the first-order Arnoldi based ROM method, when applied through a linearised state-space transformation of the original second order equations and directly to the second order system in the case of an undamped problem.

For a single-input, single-output(SISO) second order structural-acoustic system in the time domain, it is possible to represent the coupled system in the frequency domain using Laplace transforms as:

$$s^2 \underbrace{\begin{bmatrix} M_s & 0 \\ M_{fs} & M_a \end{bmatrix}}_{M_{sa}} \overbrace{\begin{Bmatrix} \tilde{u} \\ \tilde{p} \end{Bmatrix}}^{\tilde{q}(s)} + s \underbrace{\begin{bmatrix} C_s & 0 \\ 0 & C_a \end{bmatrix}}_{C_{sa}} \overbrace{\begin{Bmatrix} \tilde{u} \\ \tilde{p} \end{Bmatrix}}^{\tilde{q}(s)} + \underbrace{\begin{bmatrix} K_s & K_{fs} \\ 0 & K_a \end{bmatrix}}_{K_{sa}} \overbrace{\begin{Bmatrix} \tilde{u} \\ \tilde{p} \end{Bmatrix}}^{\tilde{q}(s)} = \mathbf{f}_{sa}\, \mu(s) \tag{4a}$$

where the output measurement vector is given by,

$$y(s) = \mathbf{l}^T \overbrace{\begin{Bmatrix} \tilde{u} \\ \tilde{p} \end{Bmatrix}}^{\tilde{q}(s)} \tag{4b}$$

and where M_s is the structural mass matrix, M_a is the acoustic mass matrix; K_s is the structural stiffness matrix, K_a is the acoustic stiffness matrix; M_{fs} is the coupling mass matrix, and K_{fs} is the coupling stiffness

matrix. $\tilde{u}$ denotes the structural displacements, and $\tilde{p}$ denotes the nodal pressures in the fluid domain. Finally, $s = j\omega$, with $j = \sqrt{-1}$ and $\omega \geq 0$. Here, $\tilde{q}(s)$ and hence $\tilde{u}$, $\tilde{p}$, $\mu(s)$, $y(s)$ are the Laplace transforms of $q(t)$ and hence u, p, $\mu(t)$ and $y(t)$ respectively. $\mathbf{f}_{sa}$ is the single-input structural-acoustic input distribution vector, and $\mathbf{l}^T$ is the output scattering vector to restore the desired state outputs.

Equations (4a and 4b) can then be re-written in terms of combined structural-acoustic matrices to give:

$$s^2\ [M_{sa}]\ \tilde{q}(s) + \ s\ [C_{sa}]\ \tilde{q}(s) + [K_{sa}]\ \tilde{q}(s) = \mathbf{f}_{sa}\ \mu(s) \tag{5a}$$

$$y(s) = \mathbf{l}^T \tilde{q}(s) \tag{5b}$$

Hence the input $\mu(s)$ and the output $y(s)$ of Equations (5a and 5b) in the frequency domain are related by the *transfer function* of the second order structural-acoustic system, which is then given by:

$$h_{sa}(s) = \frac{y(s)}{\mu(s)} \tag{6a}$$

$$h_{sa}(s) = \ \mathbf{l}^T\ (\ s^2\ M_{sa}\ +\ s\ C_{sa}\ +\ K_{sa})^{-1}\ \mathbf{f}_{sa} \tag{6b}$$

Where it is assumed that K_{sa} is non-singular.

A power series expansion of Equation (6b) can be expressed as:

$$h_{sa}(s) = \ m_0\ +\ m_1 s\ +\ m_2 s^2\ +\ m_3 s^3\ +\ \ldots \tag{7a}$$

$$h_{sa}(s) = \ \sum_{z=0}^{\infty} m_z\ s^z \tag{7b}$$

where, m_z, for all $z \geq 0$ are the *low-frequency moments* of the second order, fully-coupled structural acoustic transfer function $h_{sa}(s)$. These *low-frequency moments* are the values and their subsequent derivatives of the

transfer function h_{sa} at $s = 0$. According to earlier authors, the moment [3] m_z can be expressed as an inner product between $\mathbf{l}^T$ and g_z:

$$m_z = \mathbf{l}^T g_z \quad for \;\; all \;\; z \geq 0 \tag{8}$$

where, g_z is a vector sequence, defined by a second order recurrence relationship. For the coupled structural-acoustic case this is expressed as follows:

$$g_0 = K_{sa}^{-1}\mathbf{f}_{sa} \tag{9a}$$

$$g_1 = -K_{sa}^{-1}C_{sa}g_0 \tag{9b}$$

$$g_z = -K_{sa}^{-1}(C_{sa}g_{z-1} + M_{sa}g_{z-2}) \tag{9c}$$

for values of $z = 2, 3, \ldots$.

The vector sequence for g_z defined above is called the input second order Krylov vector sequence, which belongs to the input second order Krylov subspace, induced by two matrices A, B and the starting vector g_0, and written as:

$$\mathcal{K}_q^{ri}(A, B, g_0) = span(g_0, g_1, g_2, g_3, \ldots g_{q-1}) \tag{10}$$

where, $A = -[K_{sa}]^{-1}[C_{sa}]$, $B = -[K_{sa}]^{-1}[M_{sa}]$.

In a similar manner, the output second order Krylov vector sequence can also be computed. In this instance the moments can be expressed as an inner product between $\mathbf{f}_{sa}^T$ and l_z:

$$m_z = \mathbf{f}_{sa}^T l_z \quad for \;\; all \;\; z \geq 0 \tag{11}$$

In this case, it is also necessary to evaluate the vector sequence l_z:

$$l_0 = K_{sa}^{-T}\mathbf{l} \tag{12a}$$

$$l_1 = -K_{sa}^{-T}C_{sa}^{T}l_0 \tag{12b}$$

$$l_z = -K_{sa}^{-T}(C_{sa}^{T}l_{z-1} + M_{sa}^{T}l_{z-2}) \tag{12c}$$

for values of $z = 2, 3, \ldots$.

The vector sequence defined above is called the output second order Krylov vector sequence. This belongs to the output second order Krylov subspace, and is induced by the two matrices A^T, B^T and the starting vector l_0, written as:

$$\mathcal{K}_q^{le}(A^T, B^T, l_0) = span(l_0, l_1, l_2, l_3, \ldots l_{q-1}) \tag{13}$$

where, $A^T = -[K_{sa}]^{-T}[C_{sa}]^T$, $B = -[K_{sa}]^{-T}[M_{sa}]^T$.

Returning to the vector sequences defined in Equations (9a, 9b, 9c, 12a, 12b and 12c), it can be seen that these form the moments of the second order, structural-acoustic transfer function. The moment matching properties of the framework described here, and its equivalence to a first order structural-acoustic system is described in [17].

3 THE SECOND ORDER ARNOLDI METHOD

For the second-order Arnoldi method, projection techniques are used for dimension reduction, in a similar manner to the projection matrix V used in standard Krylov subspaces. These projection techniques use an orthogonal

projection onto the induced right subspace $\mathcal{K}_q^{ri}(A, B, g_0)$, to construct an approximation of the original system, such that:

$$q(t) = \left\{ \begin{array}{c} u(t) \\ \\ p(t) \end{array} \right\} = V_{sa} \breve{z}(t) \ + \ \varepsilon_{sa} \tag{14}$$

where, $\breve{z}(t)$ are the generalized co-ordinates and ε_{sa} is the small approximation error introduced due to the projection to generalized co-ordinates.

For dimension reduction of practical systems, it is often desirable to approximate the original coupled system for values where $s_0 \neq 0$, or even for multiple values of $s_0 \neq 0$ (leading to second order, rational Krylov methods). In this case, the transfer function of the coupled system is written as:

$$h_{sa}(s) = \ \mathbf{l}^T \ (\ s^2 \ M_{sa} \ + \ s \ C_{sa} \ + \ K_{sa})^{-1} \ \mathbf{f}_{sa}$$

$$h_{sa}(s) = \ \mathbf{l}^T \ (\ (s - s_0)^2 \ M_{sa} \ + \ (s - s_0) \ \tilde{C}_{sa} \ + \ \tilde{K}_{sa})^{-1} \ \mathbf{f}_{sa} \tag{15}$$

and, the fully coupled, structural-acoustic matrices $[\tilde{K_{sa}}]$ and $[\tilde{C_{sa}}]$ are defined as:

$$[\tilde{K}_{sa}] = s^2 M_{sa} + s C_{sa} + K_{sa} \tag{16a}$$

$$[\tilde{C}_{sa}] = 2s M_{sa} + C_{sa} \tag{16b}$$

In this expression $[\tilde{C}_{sa}]$ is simply the first derivative of $[\tilde{K}_{sa}]$. Here, s_0 can be any user specified value, with the constraint that the matrix $[\tilde{K}_{sa}]$ is non-singular.

The low frequency moments, and thus the recurrence scheme specified in Equations (9a,9b, 9c,12a,12b, 12c) are then expressed as follows:

$$h_{sa}(s) = \ \sum_{z=0}^{\infty} \tilde{m}_z \ (s - s_0)^z \tag{17}$$

where, $\tilde{m}_z$, for all $z \geq 0$ are called the *shifted low-frequency moments* of the second order, fully-coupled structural-acoustic system defined in Equations (4a,4b). These *shifted* moments can be computed as follows:

$$\tilde{m}_z = \mathbf{l}^T \tilde{g}_z, \quad \tilde{m}_z = \mathbf{f}_{sa}^T \tilde{l}_z \qquad for \;\; all \;\; z \geq 0 \tag{18}$$

with the following recurrence schemes for $\tilde{g}_z$ and $\tilde{l}_z$:

$$\tilde{g}_0 = \tilde{K}_{sa}^{-1} \mathbf{f}_{sa} \tag{19a}$$

$$\tilde{g}_1 = -\tilde{K}_{sa}^{-1} \tilde{C}_{sa} \tilde{g}_0 \tag{19b}$$

$$\tilde{g}_z = -\tilde{K}_{sa}^{-1} (\tilde{C}_{sa} \tilde{g}_{z-1} + M_{sa} \tilde{g}_{z-2}) \tag{19c}$$

for values of $z = 2, 3, \ldots$.

$$\tilde{l}_0 = \tilde{K}_{sa}^{-T} \mathbf{l} \tag{20a}$$

$$\tilde{l}_1 = -\tilde{K}_{sa}^{-T} \tilde{C}_{sa}^T \tilde{l}_0 \tag{20b}$$

$$\tilde{l}_z = -\tilde{K}_{sa}^{-T} (\tilde{C}_{sa}^T \tilde{l}_{z-1} + M_{sa}^T \tilde{l}_{z-2}) \tag{20c}$$

for values of $z = 2, 3, \ldots$.

Most real-world problems involve values of $s_0 \neq 0$, and therefore, the *shifted* moments defined in Equation (18) are a critical objective in the dimension reduction of higher order systems.

It is well known that explicit moment matching, as a technique, exhibits numerical difficulties [11], and hence, in this work, implicit moment matching is carried out via a two-sided, second-order Arnoldi-based direct projection technique. In this case, the orthonormal projection matrices, V_{sa} and W_{sa} for *Galerkin* or *Petrov-Galerkin* type projections, which span the input and

output Krylov subspaces defined in Equations (10 and 13), defined as follows are used:

$$\mathcal{K}_q^{ri}(A, B, g_0) = span(V_{sa}) \;\; and \;\; V_{sa}^T V_{sa} = I \tag{21a}$$

$$\mathcal{K}_q^{le}(A, B, l_0) = span(W_{sa}) \;\; and \;\; W_{sa}^T W_{sa} = I \tag{21b}$$

For structural-acoustic problems these matrices are of the form $[A] = -\tilde{K}_{sa}^{-1}\tilde{C}_{sa}$, $[B] = -\tilde{K}_{sa}^{-1}M_{sa}$. With these expressions, it is now possible to apply the algorithm for *standard* Arnoldi iterations, as shown in Figures 1 and 2 to compute the basis for the given Second Order Krylov Subspace. The resulting one sided SOAR procedure (which in this work is utilized to compute the two-sided second-order Arnoldi (TS-SOAR) column matrices $V_{sa}, and\ W_{sa}$)), was first proposed by [21] and later improved and extended by [3], [4], and [19].

The iterative process described here finds two sets of orthonormal basis vectors for the induced input and output subspaces, i.e. $V_{sa}^T V_{sa} = I$ and $W_{sa}^T W_{sa} = I$, and therefore the columns of the matrix V_{sa} and W_{sa} form a basis for the induced subspace.

Having carried out this TS-SOAR process, a reduced order model can now be defined by applying the *Petrov-Galerkin* projection to the coupled higher dimensional system matrices as follows:

$$[M_{rsa}] = [W_{sa}^T]\ [M_{sa}]\ [V_{sa}],\ [K_{rsa}] = [W_{sa}^T]\ [K_{sa}]\ [V_{sa}] \tag{22a}$$

$$[C_{rsa}] = [W_{sa}^T]\ [C_{sa}]\ [V_{sa}],\ \mathbf{f}_{rsa} = [W_{sa}^T]\ \mathbf{f}_{sa},\ \mathbf{l}_{rsa}^T = \mathbf{l}^T\ [V_{sa}] \tag{22b}$$

$$[M_{rsa}]\ \ddot{z}(t) + [C_{rsa}]\ \dot{z}(t) + [K_{rsa}]\ z(t) = \mathbf{f}_{rsa}\ \mu(t) \tag{22c}$$

$$y_{rsa}(t) = \mathbf{l}_{rsa}^T z(t) \tag{22d}$$

Input: Read coupled system Matrices $[K_{sa}]$, $[M_{sa}]$, $[C_{sa}]$, $\{\mathbf{f}_{sa}\}$, $\mathbf{l}^T$, q (Number of vectors) and expansion point s_0, in this case $s_0 = (\omega_e + \omega_b)/2$; or ω_e. Form and Set: $[\tilde{K}_{sa}] = s_0^2 M_{sa} + s_0 C_{sa} + K_{sa}$ and $[\tilde{C}_{sa}] = 2s_0 M_{sa} + C_{sa}$.

Output: q Arnoldi vectors belonging to the Second order Krylov Subspace. $\mathcal{K}_q^{ri}(A, B, g_0)$. In this case, $\mathcal{K}_q^r(-\tilde{K}_{sa}^{-1}\tilde{C}_{sa}, -\tilde{K}_{sa}^{-1}M_{sa}, \tilde{K}_{sa}^{-1}\mathbf{f}_{sa})$.

[0]. Delete all linearly dependent starting vectors (if multiple) to obtain k_{st} linearly independent starting vectors.

Set $\bar{v}_1 = \frac{g_0}{\|g_0\|}$ and $p_1 = 0$ for $p_1 \in \Re^n$.

[1]. * ***for*** $i = 2, 3, .. \rightarrow q$ * ***do***

[1.1] Generate next vector: * ***if*** $i \leq k_{st}$, set $\hat{v}_i$ (below) as the i^{th} starting vector and $\hat{p}_i = 0$.

* ***else***, set $\hat{v}_i = A\bar{v}_{i-k_{st}} + Bp_{i-k_{st}}$ and $\hat{p}_i = \bar{v}_{i-k_{st}}$

[1.2] Orthogonalization: * ***for*** $j = 1 \rightarrow i$ - *1*, * ***do***

$h = \hat{v}_i^T \bar{v}_j$, $\hat{v}_i = \hat{v}_i - h\bar{v}_j$, $\hat{p}_i = \hat{p}_i - hp_j$

[1.3] Normalization and Deflation check: * ***if*** $\hat{v}_i \neq 0$ (normal case), then,

* ***do*** $\bar{v}_i = \frac{\hat{v}_i}{\|\hat{v}_i\|}$, $p_i = \frac{\hat{p}_i}{\|\hat{v}_i\|}$.

* ***else if*** $\hat{p}_i \neq 0$, $\bar{v}_i = 0$.

* ***else*** $k_{st} = k_{st} - 1$. Go to step [1.1]. * ***if*** $k_{st} = 0$, delete zero columns.

[1.4] Increase i and go to step [1.1].

[2]. Delete zero columns from deflation, discard resulting H_q and project higher dimensional system $[M_{sa}]$, $[K_{sa}]$, $[C_{sa}]$, $\{\mathbf{f}_{sa}\}$, $\mathbf{l}^T$ onto $[V_{sa}]$ to obtain reduced system matrices $[M_{rsa}]$, $[K_{rsa}]$, $[C_{rsa}]$, $\{\mathbf{f}_{rsa}\}$, $\mathbf{l}_{rsa}^T$ for harmonic simulation.

Fig. 1 Algorithm 1 Set-up for SISO/SICO Second Order Arnoldi (SOAR) Process with multiple starting vectors [3,4,5].

Here *rsa* denote the reduced structural-acoustic matrices. It is worth noting that the goal of dimension reduction i.e. reduction of the system matrices from $N \times N \longrightarrow q \times q$ is now achieved, and the system described in Equations

[1]. *Initialization:* Read coupled structural-acoustic matrices, select appropriate Input and Output Krylov Subspaces: $\mathcal{K}_q^r(A, B, g_0)$, $\mathcal{K}_q^l(A^T, B^T, l_0)$ and expansion points.

Form and Set: $[\tilde{K}_{sa}]$, $[\tilde{C}_{sa}]$ as in Figure 1.

[2]. *Generate Projection Matrices:* Use the SOAR Algorithm (Figure 1) *do:

[2.1] $\mathcal{K}_q^{ri}(A, B, g_0)$: Apply $A = [-\tilde{K}_{sa}^{-1}\tilde{C}_{sa}]$, $B = [-\tilde{K}_{sa}^{-1}M_{sa}]$ and $g_0 = [\tilde{\mathrm{K}}_{sa}^{-1}]\{\mathbf{f}_{sa}\}$ to compute $[V]$.

[2.2] $\mathcal{K}_q^{le}(A^T, B^T, l_0)$: Apply $A^T = [-\tilde{K}_{sa}^{-T}]\ [\tilde{C}_{sa}^T]$, $B^T = [-\tilde{K}_{sa}^{-T}]\ [M_{sa}^T]$ and $l_0 = [\tilde{K}_{sa}^{-T}]\{\mathbf{l}\}$ to compute $[W]$.

[3]. *Apply Projection:* Use generated column matrices: $[V_{sa}]$ and $[W_{sa}]$ and apply the *Galerkin-Petrov* projection: $\prod = [V_{sa}]\ [W_{sa}]^T$ to obtain the *structure preserving* ROM matrices: $[M_{rsa}]$, $[C_{rsa}]$, $[K_{rsa}]$,$\{\mathbf{f}_{rsa}\}$ and $\mathbf{l}_{rsa}^T$for reduced harmonic or transient simulation.

Fig. 2 Algorithm 2 Higher-level, complete set-up for SISO Two Sided Second Order Arnoldi (TS-SOAR) Process.

(22c, 22d) is now ready for the modelling of reduced harmonic or transient problems.

Hence a reduced order transfer function can now be defined about any specified expansion point, s_0, as described by Bai et al [3]:

$$h_{rsa}(s) = \mathbf{l}_{rsa}^T\ (\ (s - s_0)^2\ M_{rsa}\ +\ (s - s_0)\ \tilde{C}_{rsa}\ +\ \tilde{K}_{rsa})^{-1}\ \mathbf{f}_{rsa} \qquad (23)$$

Indeed, it can be shown that the reduced transfer function can be written as:

$$h_{rsa}(s) = \mathbf{l}_{rsa}^T\ (\ s^2\ M_{rsa}\ +\ s\ C_{rsa}\ +\ K_{rsa})^{-1}\ \mathbf{f}_{rsa} \qquad (24)$$

Subsequently, the first q low frequency shifted moments about any given expansion point s_0 of the original (h_{sa}) and reduced order transfer function (h_{rsa}) are the same.

It should be noted that although the shifted matrix triple ($M_{sa},\ \tilde{C}_{sa},\ \tilde{K}_{sa}$) is used to generate the projection matrices V_{sa}, W_{sa}, the reduced order model is computed by projection onto the original higher dimensional system matrices ($M_{sa},\ C_{sa},\ K_{sa}$). The use of such modified system matrices in dimension reduction is called *structure preserving dimension reduction*, since it essentially preserves the original second order structure of the problem.

4 NUMERICAL TEST CASE 1: ABAQUS BENCHMARK PROBLEM

In order to evaluate the performance of the second order Arnoldi TS-SOAR method, a previously-reported structural-acoustic benchmark problem, which has been analysed using ABAQUS software, will be implemented, and analyses using one-sided Arnoldi, as well as performing the computation using two-sided second-order Arnoldi.

The problem consists of a semicircular shell and fluid mesh of radius 2.286 m. A point load of magnitude 1.0 N is applied to the shell along the axis of symmetry, as shown in Figure 3. The shell is 0.0254 m in thickness and has a Young's modulus of 206.8 GPa, a Poisson's ratio of 0.3, and a mass density, ρ_s, of 7800.0 kg/m^3. The acoustic fluid has a density, ρ_f, of 1000 kg/m^3 and a bulk modulus, κ_f, of 2.25 GPa. The benchmark problem is undamped.

The response of the coupled system is calculated for frequencies ranging from 100 to 1000Hz in 1Hz increments. The displacement amplitude at the coupled driving point is the primary state variable of interest. The problem is also described in the ABAQUS Benchmark manual [1,20]. The solution presented here compares analytical solutions with the coupled and uncoupled modal expansion solutions obtained utilizing ABAQUS implemented modal reduction procedures ie the Coupled Lanczos (CL) procedure, and the popular automated component mode method: Automated Multi-Level Substructuring (AMLS). In previous works by the authors [17,14], it has been demonstrated that when compared to the analytical results, the ABAQUS modal solutions (CL and AMLS) and the one-sided and two-sided Arnoldi projection methods are in good agreement over the entire frequency range (100-1000Hz) for the undamped problem. [1].

The point load presents a more challenging problem physically in the modal projection, because the single entry in the FE load vector maps to a full vector in the reduced problem, but this representation is truncated at the specified number of vectors.

For the structural damping case, three different values of β are considered. These are given in Table 1. These models result in an explicit participation of $[C_{sa}]$ and *direct-inversion* cannot be avoided. For dimension reduction, the TS-SOAR process is used for the resulting coupled higher dimensional sys-

[1] Note that the one-sided and two-sided Arnoldi process for the undamped problem does not take into account the explicit participation of the damping matrix

tem. The aim of using different expansion points for each of the damped test cases is to observe the effects of moment matching and its resulting accuracy at different frequencies and for different damping values.

Table 1 Structural Damping values and Expansion point for TS-SOAR for the ABAQUS benchmark problem.

Damped Test Cases	**Damping Value**	**Expansion Point**
Low Damping [T_{ld}]	β=5.0E-06	900Hz / 900Hz
Moderate Damping [T_{md}]	β=1.0E-05	1000Hz / 1000Hz
High Damping [T_{hd}]	β=2.0E-05	750Hz / 750Hz

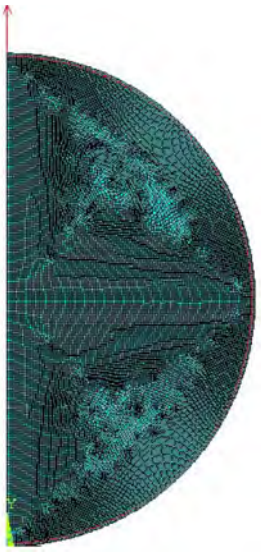

Fig. 3 Test Case No. 1: Benchmark coupled structural-acoustic model.

The generation of the reduced order model (ROM) in practice, consisted of four different steps. First, the higher dimensional model was generated in

ANSYS, and an ANSYS static solution, combined with partial solve [2] was issued to write out the relevant structural-acoustic database files. Next, an open source C++ code *dumpmatrices* [18] was used to extract the higher dimensional mass and stiffness matrices. The higher dimensional model was then read using Mathematica [23], and order reduction and projection performed via the Arnoldi process. The harmonic analysis of the reduced system was performed using LU decomposition in the Mathematica/Matlab [13] environment. The linearly damped computations described in this paper were performed on a Windows XP, Pentium 4, 3.2GHz, 2GB RAM machine. Note that the computational times in the tables may change slightly according to the condition of the computer and hardware parameters such as the reading and writing rates of the hard disk drives and the number of processes running during the analysis.

4.1 COMPUTATIONAL RESULTS AND DISCUSSION

The coupled receptance transfer function (normal structural displacement divided by input structural force) predicted by ANSYS Direct, and by the Two-Sided Second order Krylov-Arnoldi [TS-SOAR] projection for the three sub-test cases with different damping values are given in Figures 4,7, and 10.

To compare the transfer functions, a *local error* for individual states is computed, as given in [6], and defined as:

$$\breve{\hbar}_{rsa}(s) = \frac{|H(s) - H_{rsa}(s)|}{|H(s)|} \tag{25}$$

This is calculated for all values of s used for the higher dimensional model and the ROM[2]. A comparison of these local error quantities defined by Equation (25), for the TS-SOAR projection for the coupled driving point displacement amplitudes are shown in Figures 5, 8, and 11.

In order to calculate the optimum number of vectors required for convergence, two different convergence models were used. In the first convergence model, a *true error* between the two models for all states was computed as follows:

$$\vartheta_{rsa}(s) = \frac{\parallel H(s) - H_{rsa}(s) \parallel}{\parallel H(s) \parallel} \tag{26a}$$

$H(s)$ corresponds to the original transfer function, given by, $H(s) = L^T(s^2 M_{sa} + K_{sa})^{-1} F_{sa}$, and $H_{rsa}(s)$ is the reduced order transfer function.

For the second convergence model, a *relative error* between two successive reduced order models q and $q+1$ can be defined as:

$$\hat{\vartheta}_{rsa}(s) = \frac{\parallel H_{rsa}(s) - H_{rsa+1}(s) \parallel}{\parallel H_{rsa}(s) \parallel} \tag{26b}$$

For the coupled driving point displacement, the results of the two convergence models are shown in Figures 6, 9, and 12. The convergence plots suggest that it is not possible to increase the accuracy of the TS-SOAR approach beyond the use of 110 TS-SOAR generated vectors. This means that the reduced order system is of order 110 as opposed to the original higher dimensional model of order 23412.

[2] Throughout this work, absolute values for the numerator and denominator are utilized for error computations.

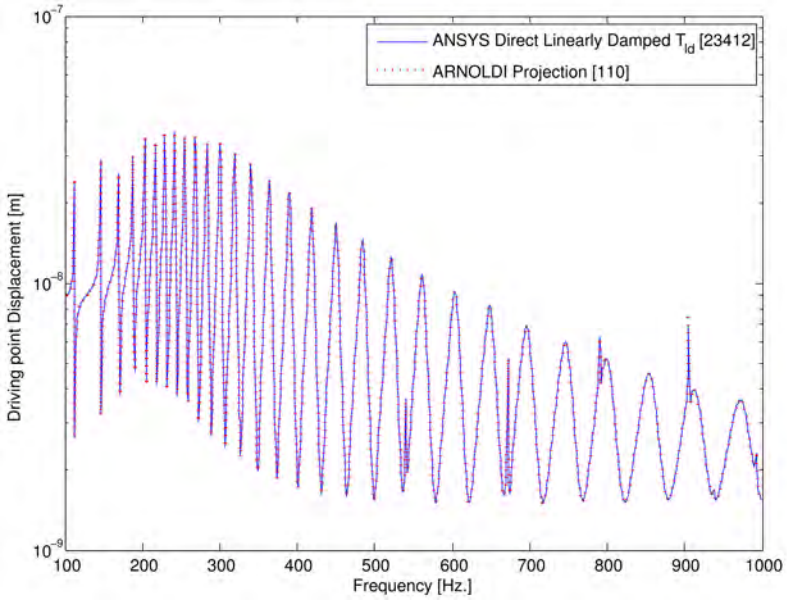

Fig. 4 A comparison between ANSYS direct inversion and Two-Sided Second order Arnoldi (TS-SOAR) predictions of driving point displacement for the model with low damping, T_{ld}.

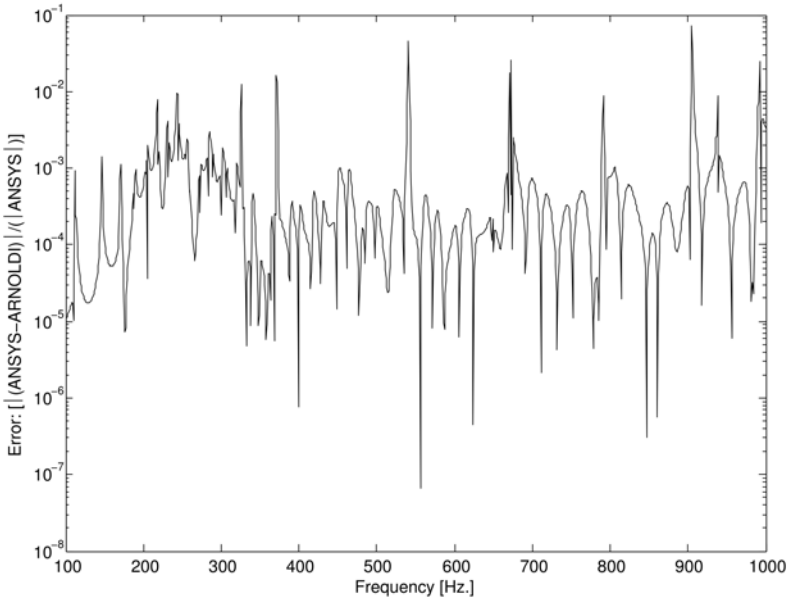

Fig. 5 Error Plot: ANSYS direct inversion and Two-Sided Second order Arnoldi (TS-SOAR) predictions for structural driving point displacement for the model with low damping T_{ld}.

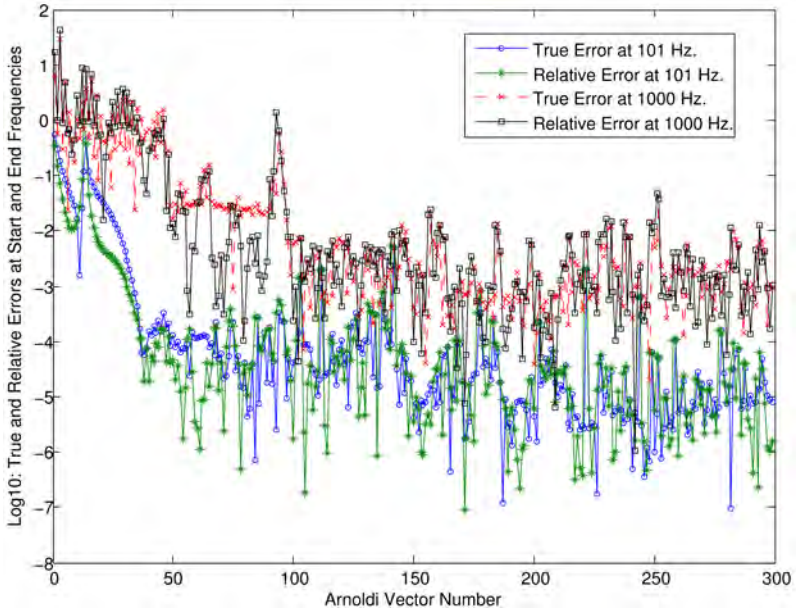

Fig. 6 Convergence Plot: Two-Sided Second order Arnoldi (TS-SOAR) convergence at 101Hz and 1000Hz for the model with low damping, T_{ld}.

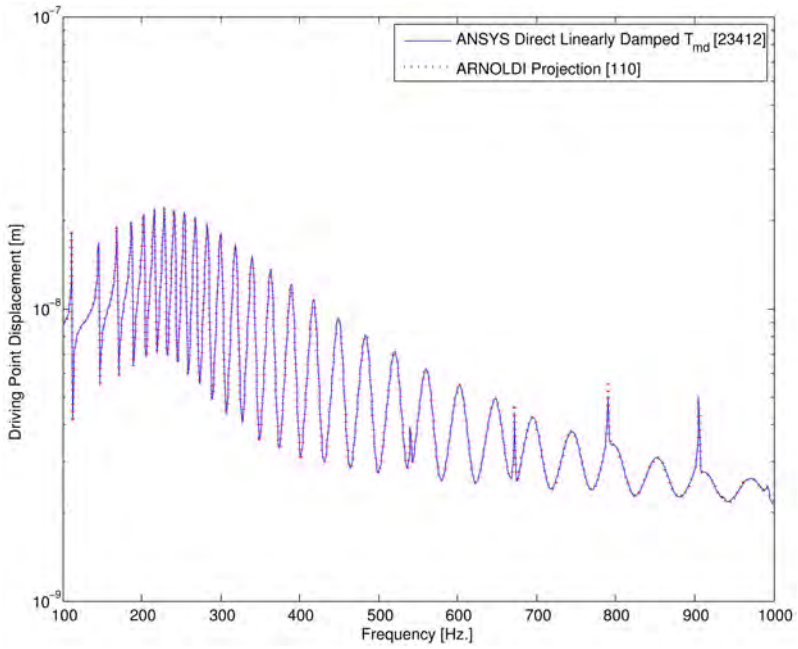

Fig. 7 A comparison between ANSYS direct inversion and Two-Sided Second order Arnoldi (TS-SOAR) predictions of driving point displacement for the model with medium damping, T_{md}.

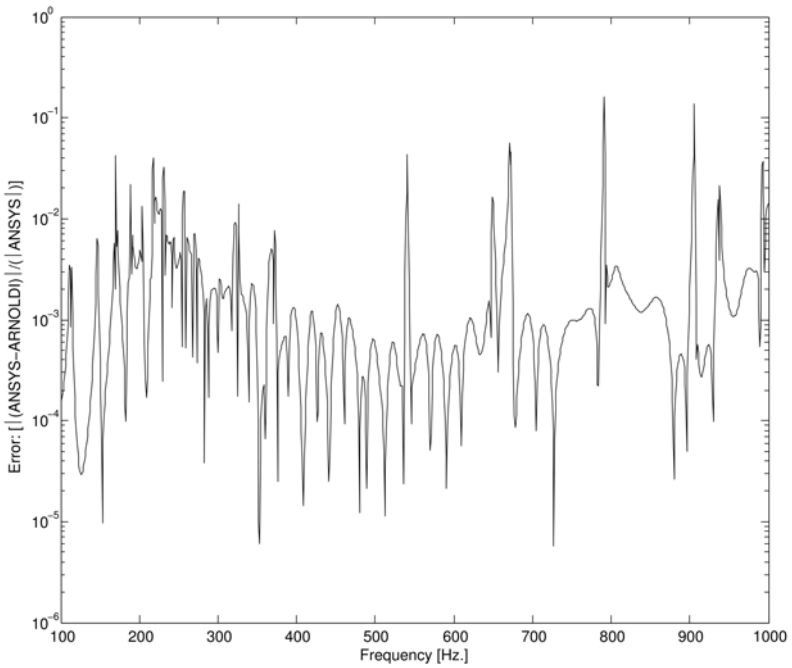

Fig. 8 Error Plot: ANSYS direct inversion and Two-Sided Second order Arnoldi (TS-SOAR) predictions for structural driving point displacement for the model with medium damping, T_{md}.

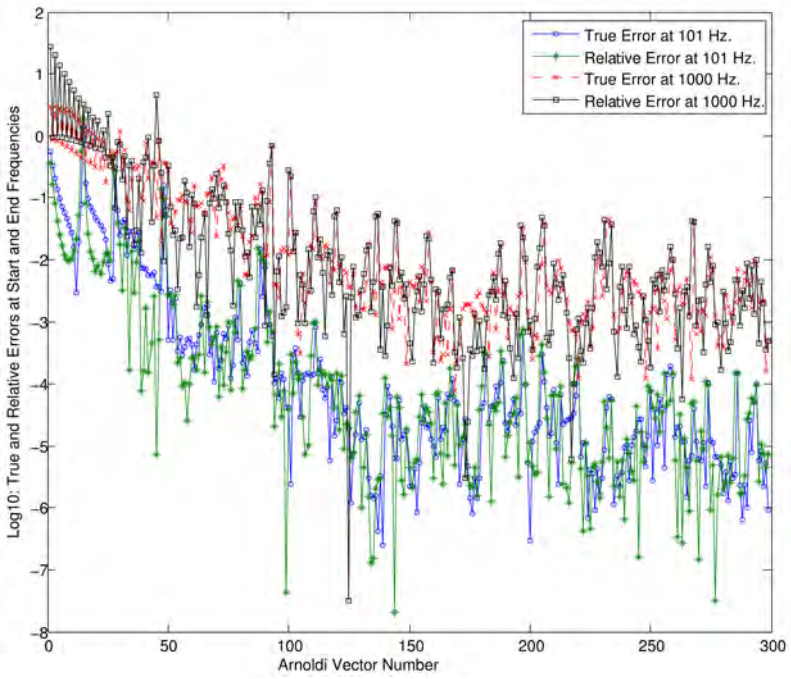

Fig. 9 Convergence Plot: Two-Sided Second order Arnoldi (TS-SOAR) convergence at 101Hz and 1000Hz for the model with medium damping, T_{md}.

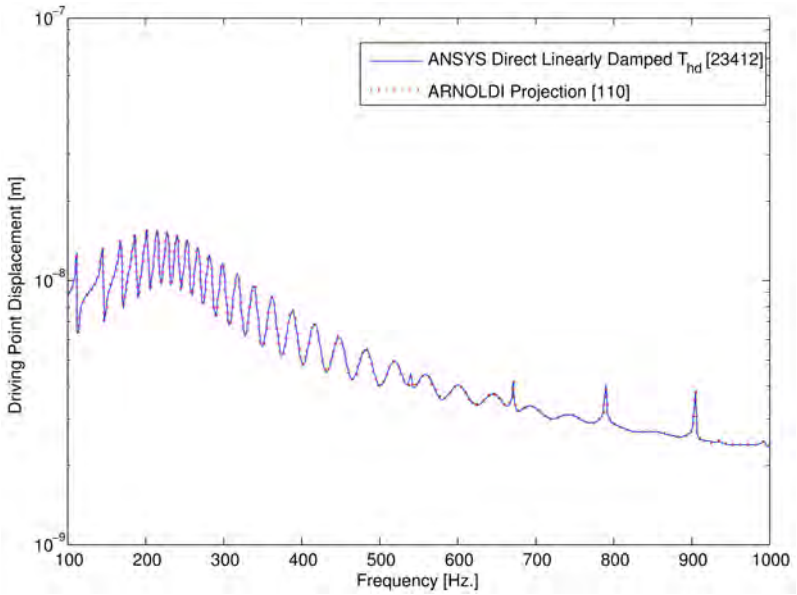

Fig. 10 A comparison between ANSYS direct inversion and Two-Sided Second order Arnoldi (TS-SOAR) predictions of driving point displacement for the model with high damping, T_{hd}.

The computational times for the solutions obtained using ANSYS direct, and using the reduced order method, based on the proposed TS-SOAR framework is shown in Table 2. From this, it can be seen that the Krylov-Arnoldi projection saves computational time of around 97%.

Table 2 A comparison of computational times for damped test cases.

Test Case	**ANSYS Direct**	**ROM via TS-SOAR**	**Time Reduction**
T_{ld}	6413 s	75 s	98.83%
T_{md}	6004 s	75 s	98.75%
T_{hd}	6319 s	176 s	97.21%

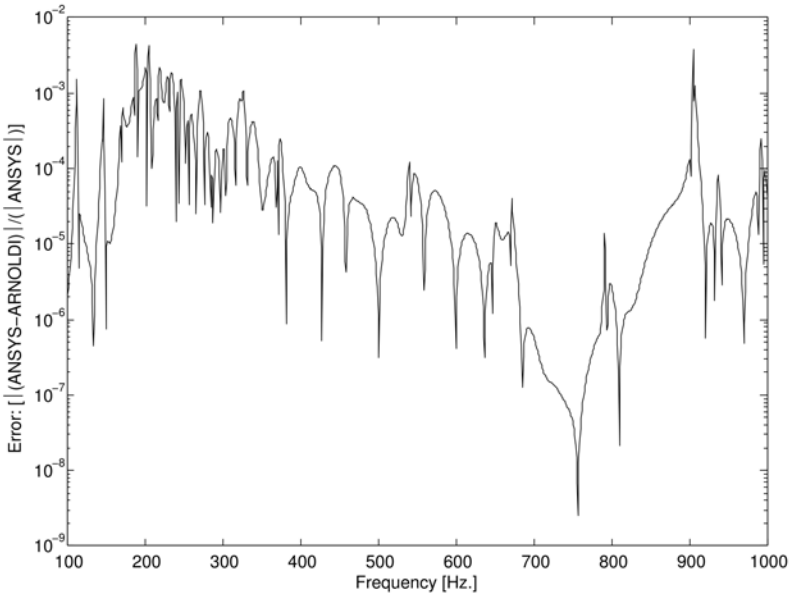

Fig. 11 Error Plot: ANSYS direct inversion and Two-Sided Second order Arnoldi (TS-SOAR) predictions for structural driving point displacement for the model with high damping, T_{hd}.

5 NUMERICAL TEST CASE 2: CYLINDER ENCLOSING AN AIR FILLED CAVITY

A steel cylinder is considered as the second test case to test the accuracy and efficiency of the proposed Second Order Arnoldi based projection formulations. The cylinder has the following dimensions: 1.01 m long, 0.18256 m radius, and 0.001219 m thick, and is made from steel with the following mechanical properties: Youngs modulus E_s= 200 GPa, mass density ρ_s=7800kg/m^3, Poissons ratio υ_s=0.33. The cavity is filled with air having the following properties: speed of sound c=343m/s, and mass density ρ_c=1.2kg/m^3. The coupled system is excited using a normal unit point load

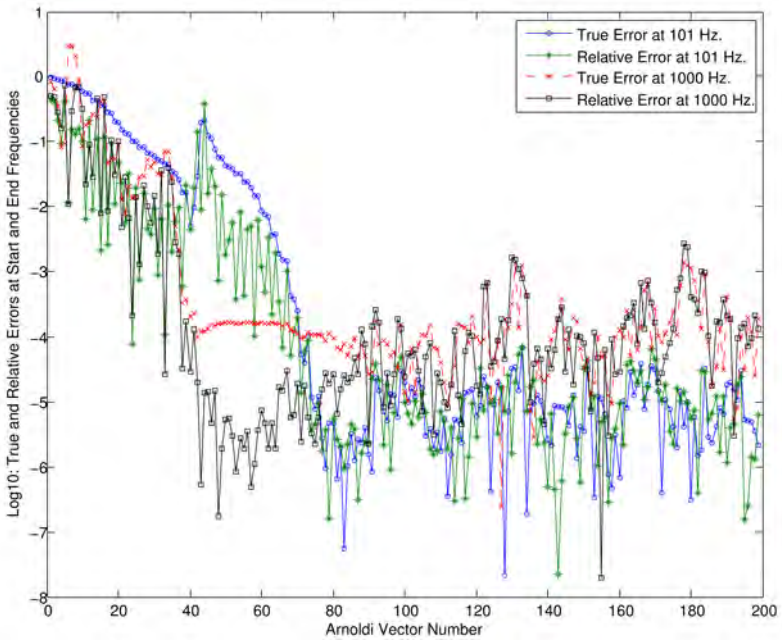

Fig. 12 Convergence Plot: Two-Sided Second order Arnoldi (TS-SOAR) convergence at 101Hz and 1000Hz for the model with high damping, T_{hd}.

defined in Figure 14. A description of this test case can also be found in [22, 7], where it is reported that the test case is *strongly coupled*.

The cylinder is discretized using 32 4-node quadrilateral ANSYS SHELL63 elements along the perimeter and 22 elements along the length. The cavity is discretized using 4-node one DOF pressure elements (ANSYS FLUID30), with 32 mesh divisions along the perimeter, 22 mesh divisions along the length, and 15 mesh divisions along the diameter. The desired output quantity considered for this test case is the fluid nodal pressure values at the centre of the cylinder. The damping values used in the test cases are given in Table 3.

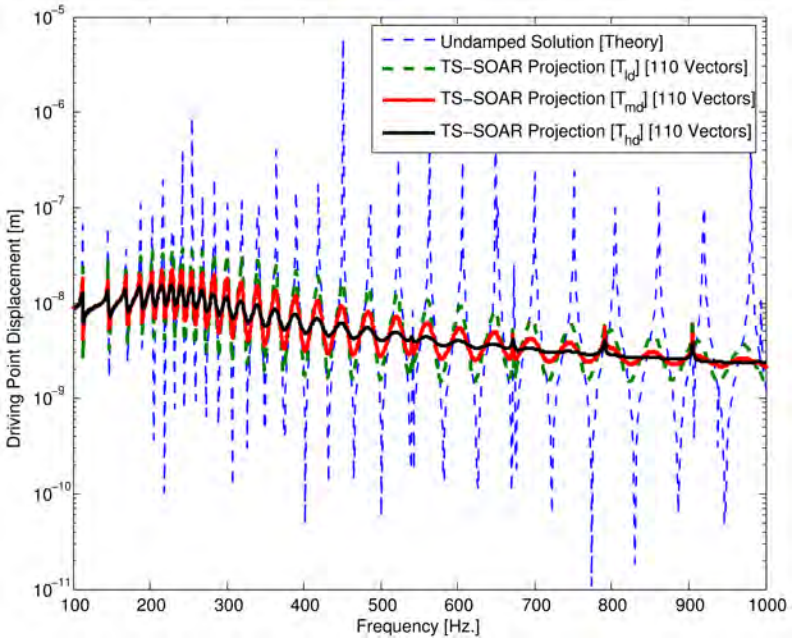

Fig. 13 A comparison between undamped and damped solutions obtained by analytical solution [20, 1] and Two-Sided Second order Arnoldi (TS-SOAR) procedure for the three values of damping, T_{ld}, T_{md}, T_{hd}.

Table 3 Damping values and Expansion points for Second Order Arnoldi Process for Test Case No.2

Damped Test Cases	**Damping Value**	**Expansion Point**
Low damping [TC2$_{FD1}$]	β=5.0E-05	600 / 600 Hz
High damping [TC2$_{FD2}$]	β=7.0E-05	600 / 600Hz

For the two damping models, the SISO Two-Sided Second Order Arnoldi (TS-SOAR) and the first order one-sided Arnoldi framework were used to generate the reduced order models. These were compared with models solved directly in ANSYS.

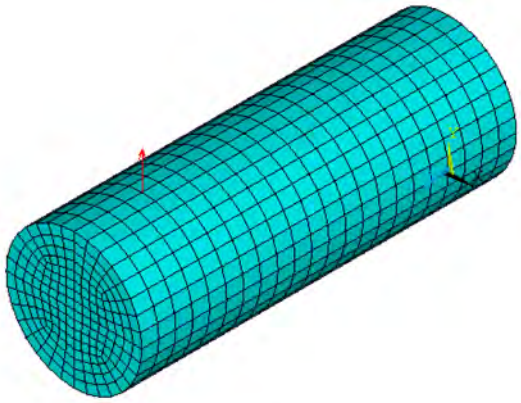

Fig. 14 Test Case No. 2: FE mesh for clamped air-filled cylindrical cavity

5.1 COMPUTATIONAL RESULTS AND DISCUSSION

For the model with low damping [TC4$_{FD1}$], ie with β=5.0E-05, the noise transfer function at the center of the cylinder is shown in Figure 15. The local error plot (Figure 16) and the convergence plot (Figure 17) shows that no accuracy is lost by generating the ROM via TS-SOAR approach and that no more than 40 Arnoldi generated vectors (for each subspace) are required for the solution state to be considered converged.

For the structural acoustic model with β_j^m=7.0E-05, [TC4$_{FD2}$], it can be observed from Figure 18 that both the linearization (with OSA) and TS-SOAR projection framework generate accurate reduced order models. However, to achieve convergence, the first order transformed model requires 200 Arnoldi generated vectors, as shown in Figure 20, (due to the introduced scaling to a first order system), whereas, for the TS-SOAR framework, a ROM of dimension 40 provides the same accuracy for the considered output.

For the linearization approach, an expansion point of 600Hz ($2 \times \pi \times 600$) has been chosen for the analysis. The local error quantities shown in Figure 19, are both so small as to be considered negligible. However, these do in fact show that the one-sided Arnoldi approach gives a higher degree of accuracy over the entire frequency range, whereas the two-sided Arnoldi method gives a reduced order model with higher accuracy around the chosen expansion point (600Hz).

This indicates that the second-order Arnoldi method shows advantages over the one-sided method, in terms of the smaller number of Arnoldi generated vectors and hence dimension of the reduced order model to give the same accuracy, but also in terms of improved local accuracy around the chosen expansion point. The two-sided Arnoldi method also provides significant benefits in terms of structure preservation and the ability to relate to the original structure, in comparison with the one-sided Arnoldi technique, which requires linearization, and does not preserve the original structural model.

The computational times required to solve the higher dimensional problem via ANSYS direct and the Arnoldi-based dimension-reduction techniques are given in Table 4. The time required for reduced order modelling via Arnoldi is a combination of the time required to generate the Arnoldi vectors, to project the system to second order form and perform a harmonic analysis on the reduced order model. It can be observed that the computational times are very similar for the different versions of the test cases. The

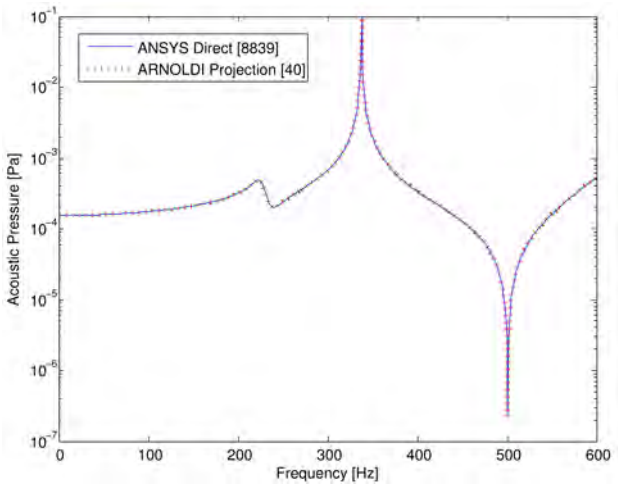

Fig. 15 Predicted Noise Transfer Function (NTF) using ANSYS direct and the two-sided TS-SOAR projection (40 Arnoldi Vectors) for the fluid node at the centre of the cylindrical cavity model [$TC4_{FD1}$] with β=5.0E-05.

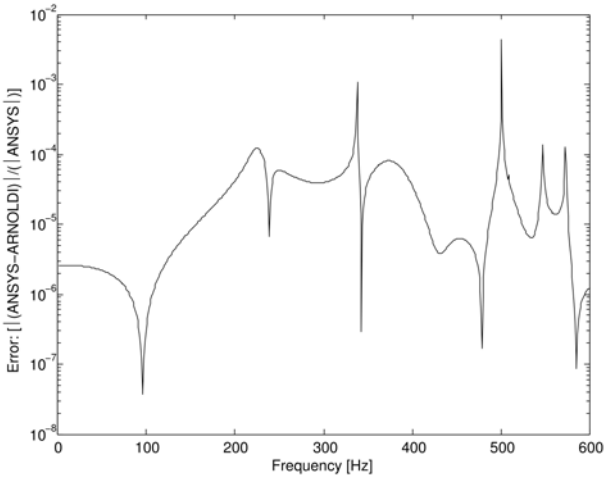

Fig. 16 Local Error Plot for two-sided TS-SOAR Arnoldi projection for the fluid node at the centre of the cylindrical cavity with β=5.0E-05 (40 Arnoldi Vectors).

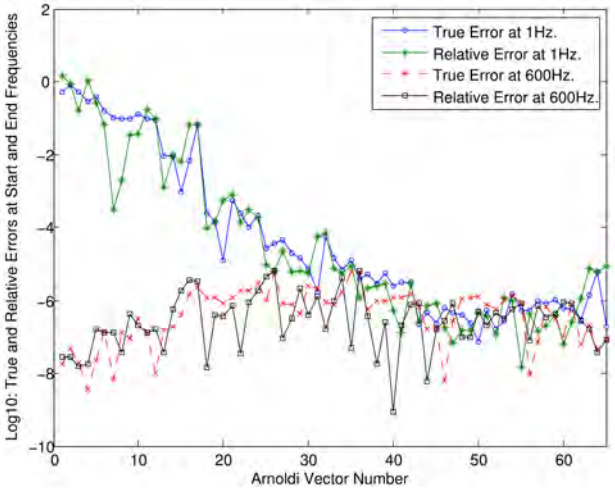

Fig. 17 Convergence plot for two-sided TS-SOAR Arnoldi projection for the fluid node at the centre of the cylindrical cavity with β=5.0E-05 (40 Arnoldi Vectors).

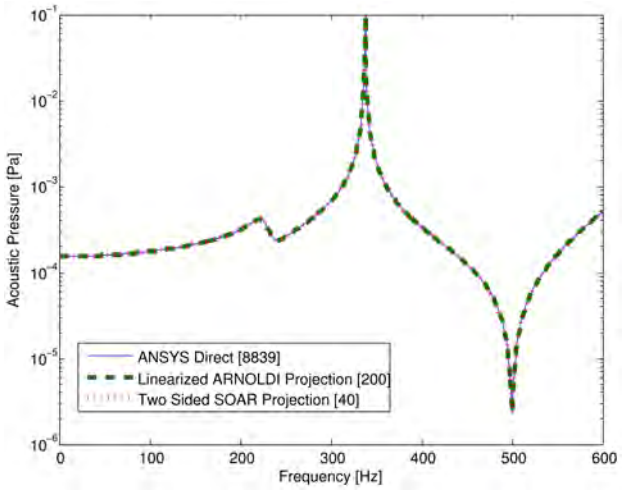

Fig. 18 Predicted Noise Transfer Function (NTF) using ANSYS direct, the linearized one-sided Arnoldi (OSA - 200 vectors), and the two-sided TS-SOAR Arnoldi projection (40 Arnoldi Vectors) for the fluid node at the centre of the cylindrical cavity model [TC4$_{FD2}$] with β=7.0E-05.

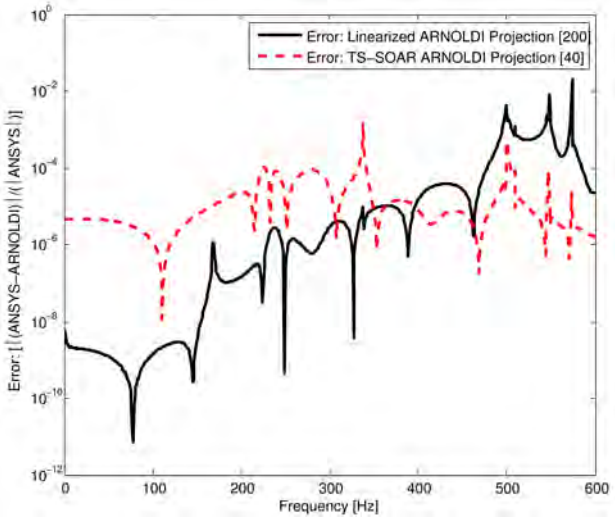

Fig. 19 Local Error quantities for reduced order models generated via the one-sided Arnoldi (OSA), and the two-sided TS-SOAR Arnoldi projection for the fluid node at the centre of the cylinder with β=7.0E-05.

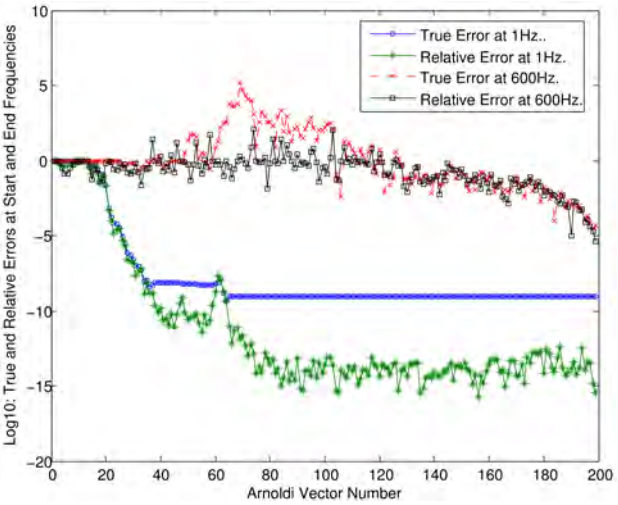

Fig. 20 Convergence plot for moment-matching one-sided Arnoldi (OSA) for the fluid node at the center of the cylinder with β=7.0E-05 (40 Arnoldi Vectors).

one-sided Arnoldi approach (for Test Case: $TC4_{FD2}$) results in a drop of computational efficiency (by around 3%) due to the increased dimension of the equivalent system, and the fact that more Arnoldi vectors were required to achieve convergence of the solution state.

Table 4 A comparison of computational times for undamped and damped test cases.

Test Case	**ANSYS Direct**	**ROM via Arnoldi**	**Time Reduction**
[$TC4_{FD1}$]	4201 s	95.1 s	97.7%
[$TC4_{FD2}$]	4719 s	88.2 s	98.1%
Linearization		160.5 s	96.5%

6 CONCLUSION

In this paper, two fully-coupled structural-acoustic models have been analysed using the two-sided second-order Arnoldi based method of model order reduction. The first case was an air-filled steel sphere, with a point load applied to the shell along the axis of symmetry. The second case was an air-filled, steel cylinder with clamped ends, which was excited by a load normal to the surface of the shell.

The models were also analysed using the direct inversion technique in ANSYS, and the cylindrical model was analysed using the one-sided Arnoldi based reduced order modelling technique. True and relative error functions were calculated between the Arnoldi and direct ANSYS models, and conver-

gence models were also compared. Solution times for the models and techniques were also compared.

Structural damping was also considered in this work in the form of proportional damping, with different values of damping. Although this results in an explicit participation of the damping matrix, which requires direct inversion, there is no reduction in the ROM efficiency as expressed by the error functions and the solution times.

The results demonstrated a significant increase in efficiency of the two-sided Arnoldi method, in comparison with the one-sided Arnoldi method, although both methods showed an improvement of computational efficiency of two orders of magnitude in comparison with the Direct method in ANSYS. The two-sided Arnoldi method required a smaller number of convergence vectors, and gave better local accuracy around the expansion points. Additionally, the underlying second order structure of the original problem is preserved. For a comparison with mode-based (coupled and uncoupled) methods for strongly coupled problems, the reader is reffered to [17]. As a concluding remark, it is worth noting that, the ROM methods discussed in this paper are particularly suitable for low to mid frequency vibro-acoustic design and optimization, where there is relatively low modal density.

Acknowledgements

The authors wish to acknowledge the Engineering and Physical Sciences Research Council (EPSRC GR/S27245/01) for the grant project under which this research was carried out. The authors also acknowledge the support of

Jeffrey L. Cipolla (Simulia Corporation formerly ABAQUS Inc.), T. Bharj (Ford Motor Company U.K), M. Birrell (BI-Composites, U.K), R Davidson (Crompton Technology, U.K), M. Collier (Hodgson and Hodgson, U.K), A. Atkins (Siemen's Magnet Technology, U.K) and M. Burnett (Motor Industry Research Association, U.K) who were industrial collaborators in the project.

References

1. ABAQUS. *V6.5 Theory and Benchmark Manual*. http://www.simulia.com/; Accessed on: 01/02/2005, 2005.
2. ANSYS. *V10 Theory Manual*. http://www.ansys.com; Accessed on: 06/12/2005, 2005.
3. Z. J. Bai, K. Meerbergen, and Y.F. Su. Arnoldi methods for structure preserving dimension reduction of second-order dynamical systems. *Dimension Reduction of Large-Scale Systems, Lecture Notes in Computer Science and Engineering*, 45:173–189, 2005.
4. Z. J. Bai and Y.F. Su. Dimension reduction of large-scale second-order dynamical systems via a Second-Order Arnoldi method. *SIAM Journal on Scientific Computing*, 26(5):1692 – 1709, 2005.
5. Z. J. Bai and Y.F. Su. SOAR: A Second-order Arnoldi method for the solution of the quadratic eigenvalue problem. *SIAM Journal on Matrix Analysis and Applications*, 26(3):640–659, 2005.
6. Tamara Bechtold, Evgenii B Rudnyi, and Jan G Korvink. Error indicators for fully automatic extraction of heat-transfer macromodels for mems. *Journal of Micromechanics and Microengineering*, 15(3):430, 2005.
7. S. Boily and F. Charron. The vibroacoustic response of a cylindrical shell structure with viscoelastic and poroelastic materials. *Journal of Applied Acoustics*, 58(2):131–152, 1999.
8. A. Craggs. The transient response of coupled acousto-mechanical systems. *NASA Contractor Report*, CR1421:1–82, 1969.

9. A. Craggs. The transient response of a coupled plate-acoustic system using plate and acoustic finite elements. *Journal of Sound and Vibration*, 15:509–528, 1971.

10. A. Craggs. An acoustic finite element approach for studying boundary flexibility and sound transmission between irregular enclosures. *Journal of Sound and Vibration*, 30:343–357, 1973.

11. Roland W. Freund. Model reduction methods based on Krylov subspaces. *Acta Numerica*, 12:267–319, 4 2003.

12. S. Marburg. Developments in structural-acoustic optimization for passive noise control. *Archives of the Computational Methods in Engineering*, 9(4):291–370, 2002.

13. Matlab. *Matlab Manual V7.0.4*. http://www.matlab.com; Accessed on: 12/03/2006, 2006.

14. R. S. Puri, D. Morrey, and J. L. Cipolla. A comparison between One-sided and Two-sided Arnoldi based model order reduction techniques for fully coupled structural acoustic analysis. In *153rd Meeting of the Acoustical Society of America, The Journal of Acoustical Society of America*, volume 121, page 3097, 2007.

15. R. Srinivasan Puri and Denise Morrey. A Krylov—Arnoldi reduced order modelling framework for efficient, fully coupled, structural—acoustic optimization. *Struct. Multidiscip. Optim.*, 43(4):495–517, April 2011.

16. R. Srinivasan Puri, Denise Morrey, Andrew J. Bell, John F. Durodola, Evgenii B. Rudnyi, and Jan G Korvink. Reduced order fully coupled structural acoustic analysis via implicit moment matching. *Applied Mathematical Modelling*, 33(11):4097 – 4119, 2009.

17. R.S. Puri. *Krylov Subspace Based Direct Projection Techniques For Low Frequency, Fully Coupled, Strutural Acoustic Analysis and Optimization.* PhD thesis, School of Technology, Department of Mechanical Engineering and Mathematical Sciences, Oxford Brookes University, Oxford, UK., 2008.

18. Evgenii. Rudnyi and Jan. Korvink. Model order reduction for large scale engineering models developed in ANSYS. In Jack Dongarra, Kaj Madsen, and Jerzy Wasniewski, editors, *State of the Art in Scientific Computing*, volume 3732 of *Lecture Notes in Computer Science*, pages 349–356. Springer Berlin Heidelberg, 2006.

19. B. Salimbahrami. *Structure Preserving Order Reduction of Large Scale Second Order Models*. PhD thesis, Department of Electrical Engineering, Technische Universitaet Muenchen, Germany, 2005.

20. P. Stepanishen and D. L. Cox. Structural-acoustic analysis of an internally fluid-loaded spherical shell: Comparison of analytical and finite element modeling results. *NUWC Technical Memorandum, Newport, Rhode Island*, (00-118), 2000.

21. T. J. Su and R.R. Craig. Model reduction and control of flexible structures using Krylov vectors. *AIAA Journal of Guidance and Control Dynamics*, 14(2):260–267, 1991.

22. M. Tournour and N. Atalla. Pseudostatic corrections for the forced vibroacoustic response of a structure-cavity system. *Journal of Acoustical Society of America*, 107(5):2379–2386, 2000.

23. Wolfram. *Mathematica V5.0*. http://www.wolfram.com; Accessed on: 23/06/2005, 2003.

24. O.C. Zienkiewicz and R. Newton. Coupled vibrations of a structure submerged in a compressible fluid. *Proceedings of the International Symposium on Finite Element Techniques,Stuttgart,Germany*, 15:1–09, 1969.